ISSN : 0974 - 7486 Volume 14 Issue 2

Materials Science

An Indian Journal

Full Paper

MSAIJ, 14(2), 2016 [038-046]

Effect of different thermal treatments and hardening amounts on several physical and mechanical properties of a spheroidal graphite cast iron

Kamel Meridja, Patrice Berthod*

Institut Jean Lamour (UMR 7198), Team 206 "Surface and Interface, Chemical Reactivity of Materials" Faculty of Sciences and Technologies, University of Lorraine, B.P. 70239, 54506 Vandoeuvre-lès-Nancy, (FRANCE)

E-mail: Patrice.Berthod@univ-lorraine.fr

ABSTRACT

Several properties of cast irons may depend on the temperature history as some physical and mechanical ones. In this work the evolutions of microstructure, volume mass, compression properties and hardness resulting from different heat-treatment and cooling conditions were studied for a same initial spheroidal cast iron. Samples cut in a same ingot were subjected to austenitization then cooling at very different rates, eventually followed by medium temperature stage. Some of them were additionally compressed until reaching 800 to 1000 GPa. Their microstructure, volume mass, plastic deformation amount and hardness were characterized and compared to analyse the effects of thermal treatment and hardening in compression on the microstructure, hardness and density.

KEYWORDS

Spheroidal graphite cast iron;
Silicon;
Heat treatment;
Microstructure;
Volume mass;
Compression properties;
Hardness.

INTRODUCTION

Cast irons[1, 2] are iron-carbon alloys especially easy to shape by foundry, thanks to a melting temperature range rather low (by comparison to steels) allowing a good castability. The binary Fe-C diagrams[3] shows that a carbon content of about 4-4.5 wt.% lowers the melting point from 1535°C for pure Fe down to 1153°C in the stable diagram (austenite-graphite) and 1147°C in the metastable diagram (austenite-cementite). Cast irons poured in moulds directly after exiting the bottom part of the blast furnace[4,5] additionally contain silicon (for example 2.5 wt.%), but no other element in significant quantity. This "clean" chemical composition of the "pig iron" (i.e. cast iron resulting directly from ore reduction) allows the cast pieces solidifying according to the stable diagram if the cooling rate is not too fast. The obtained microstructure is thus constituted of austenite (pre-eutectic dendrites and eutectic, or only eutectic) and graphite (eutectic or re-eutectic and eutectic), this depending on the value of the equivalent carbon content {wt.%C + (wt.%Si + wt.%P)/3}, more precisely its position by regards to the eutectic composition. Solid state transformations near 800°C may be the eutectoid one of austenite results in ferrite and additional graphite if the solid state cooling rate is slow enough, ferritic-pearlitic and

even pearlitic if cooling is faster. Bainitic or martensitic transformations may also partly or totally occur when the piece is cooled very rapidly or water-quenched.

Without any treatment of the liquid metal prior to moulding, the shape of the structure of graphite is lamellar ("flake graphite"), coarse if solidification rate is low and fine if it is more rapid and/or if the liquid metal was inoculated before or during pouring. Other possible liquid metal treatments are desulfurization (e.g. with CaO) applied to purify the melt from the sulphur introduced with the iron ore in the blast furnace, and spheroidization by adding Mg-rich FeSi alloy in the form of powders or by immersion of Mg blocks to diminish the liquid iron contents in poison elements (S, O… down to less than at least 0.01 wt.%). After final inoculation with a FeSi powder containing nuclei for graphite (and sometimes rare earth elements), the graphite particles crystallize as nodules ("spheroidal graphite")[6].

Nodular graphite allows obtaining higher mechanical properties than flake graphite, with better strength and ductility. The mechanical properties may be thereafter rated by heat-treatments aiming to modify the matrix. Austenitization at about 1000°C may be envisaged to reinitiate the matrix before applying either a faster cooling than previously to promote ferritic-pearlitic or wholly pearlitic transformation of the matrix, or quenching for obtaining bainitic matrix (austempered ductile iron) or martensite (which can be thereafter partly softened by an ageing heat treatment). Thus, even in the single graphite-containing type of cast irons, many microstructures may be obtained[7-10].

So various microstructures of cast iron may lead to various densities, physical property which can be furthermore also influenced by permanent deformation achieved by applying stresses intense enough which may induce plastic deformation of the matrix and compressing graphite. This is the aim of this work to achieve different matrixes from a same spheroidal graphite cast iron and to deform the obtained samples, for studying first the variations of their volume mass versus the applied heat and/or mechanical treatments, as well as the recorded compression mechanical properties and the hardness in the different states.

EXPERIMENTAL

The initial material and preparation of samples to be heat-treated

An ingot of about 5cm × 5cm × 10cm of spheroidal graphite cast iron was available in the laboratory. The observation of its microstructure, illustrated (Figure 1) by an optical micrograph after Nital4 (96%.vol ethanol – 4%.vol HNO_3) etching shows that this ingot was made of a SG cast iron, containing nodular graphite but also primary cementite and pearlite.

Its chemical composition was determined by Energy Dispersion Spectrometry using a Scanning Electron Microscope (SEM) JEOL JSM 6010LA: it is composed of principally iron, carbon (not measurable with this technique) and of 2.53 wt.% of silicon.

This ingot was cut, using a precision metallographic saw, in order to obtained several cubes which were thereafter ground with SiC papers from 240-grit up to 1200-grit by keeping their cubic geometries (no smoothing of their edges and corners).

The different applied heat-treatments

Thereafter a cube was placed in a small resis-

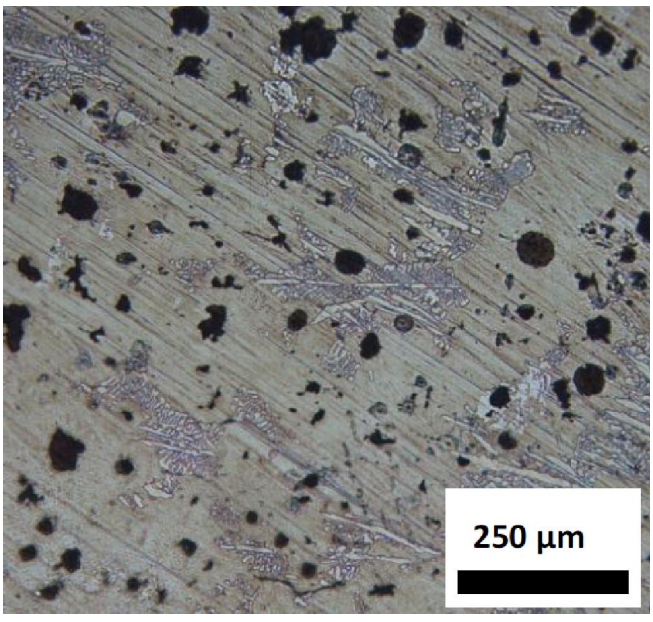

Figure 1 : Micrograph illustrating the as-cast microstructures of the re-melted then re-solidified cast irons (Nital 4 etching, optical microscope); the Si content increases from the left micrograph to the right one

tive tubular furnace (Carbolite, MTF 12/38/250, T_{max} = 1200°C) in which it was heated up to 900°C, temperature at which it was maintained during one hour to achieve total austenitization, before slowly cooling in the shutdown closed furnace.

Three other cubes were heated in the same furnace and underwent the same isothermal stage. One of these three ones was fast exited and it cooled in the laboratory air. The two other ones were instantaneously ejected and fell in room temperature water. One of them was kept in this quenched state while the other one was annealed by a heat treatment achieved in the same furnace but at 350°C only for 30 minutes before exiting for cooling in air.

All cubes were ground again (papers 600 then 1200) in order to remove the oxidation affected zone from the six faces again by keeping a perfect cubic geometry.

Volume mass determination

The geometries and dimensions of the four heat-treated samples were then controlled and measured with accuracy (geometry really cubic) while their masses were measured using a precision (±0.1mg) micro-balance, and their volume mass (densities) calculated. Thereafter the four cubes were each cut in two parallelepiped parts: a first one was kept in it present state ("before compression" or "not deformed") while the second one was subjected to elastic then plastic compressive deformation ("after compression" or "deformed").

The compression tests

The parts devoted to the compression tests were compressed using a MTS Alliance RF150 traction/compression/flexion electromechanical machine (force capacity: 150kN) equipped with two platens and a force cell (capacity: 150kN too), driven using a DELL Latitude D505 portable computer supporting the MTS Testworks 4 software. All compression runs were realized at a rate of 1mm per minute (but less than this value near the end of the tests) until reaching about 80kN. The deformed samples were thereafter ground with 1200-grit SiC papers and their new dimensions (thickness notably) measured again (electronic calliper). The plastic deformation rates were calculated from the initial and final thicknesses measured again with the electronic calliper. The two other sides were also measured again to value the new volume masses.

Microstructure control

After ultrasonic cleaning one of the six faces of each sample (not deformed or compressed) was then polished using textile disk sprayed with 1µm-hard particles containing solvent, after having smoothed the four surrounding edges and the four corresponding corners with 1200-grit SiC paper. The microstructures were observed using an optical microscope Olympus BX51, equipped with a ToupCam digital camera managed by the ToupView software, without etching to examine the graphite particles and after Nital etching (Nital4) to know the matrix nature. The initial microstructures were thus specified and the consequences of compression examined.

Macro-hardness measurements

Vickers indentations were performed using a Testwell Wolpert testing machine, under a load of 30kg. Three indentations per samples led to an average value and a standard deviation one.

RESULTS AND DISCUSSION

Microstructures of the heat-treated samples

The microstructures of the two samples cooled in furnace and in air after austenitization are illustrated by optical micrographs in Figure 2. One can see the nodular graphite in the not etched samples (partly deteriorate by grinding although that this was done in dry conditions (no water as lubricant). Nital etching allowed seeing that the microstructure is mainly ferritic (ferrite in white) but also contains some pearlite (grey) in the sample cooled in the furnace while the microstructure of the air-cooled sample is mainly composed of pearlite although ferrite is also visible. The microstructures of the two other samples, the water-quenched one and the quenched then annealed one are shown in Figure 3. Graphite is also globally nodular and the metallic matrix is martensitic. One can notice that some graphite spheroids seem hollow in their centre: it is possible that grinding did not re-

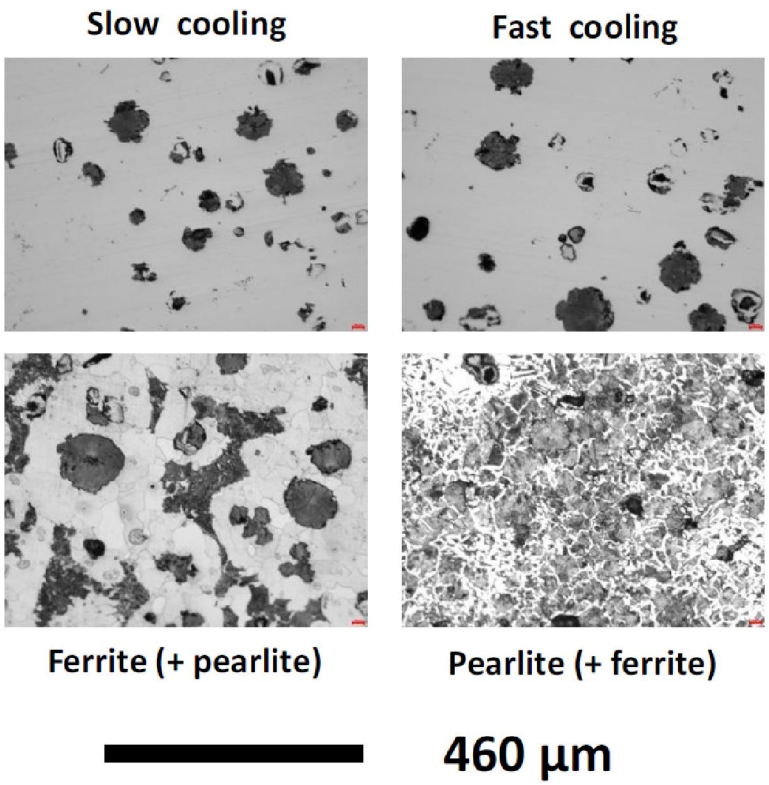

Figure 2 : Graphite structure (without etching, top) and matrix (after Nital etching, bottom) of the slowly cooled sample and of the rapidly cooled sample, (after grinding and polishing of one face of each heat-treated cube)

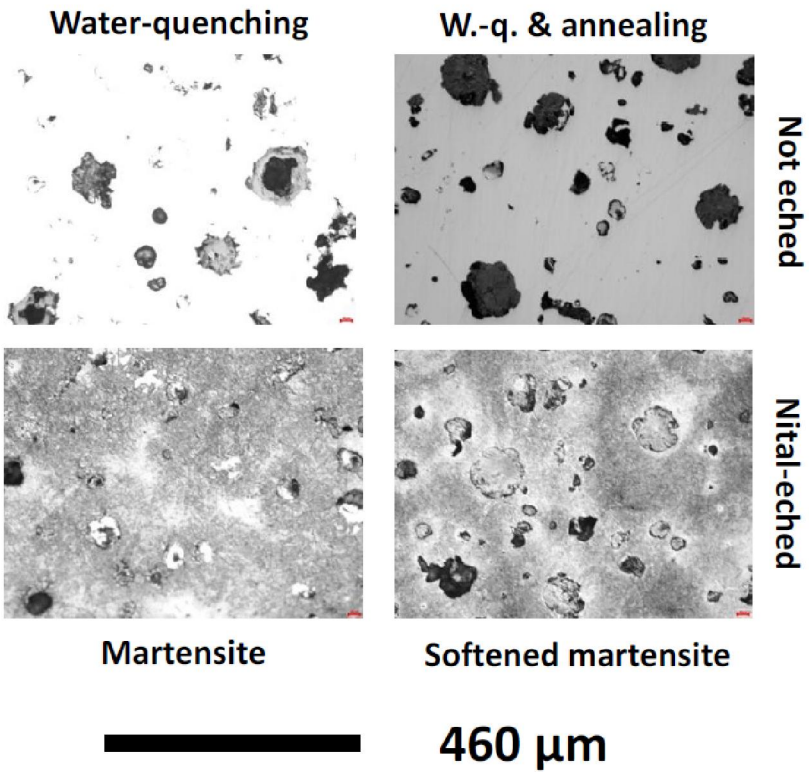

Figure 3 : Graphite structure (without etching, top) and matrix (after Nital etching, bottom) of the water-quenched sample and of the quenched then annealed sample, (after grinding and polishing of one face of each heat-treated cube)

move the whole oxidation-affected zone and locally spherical cavities quitted by graphite oxidized into gases may be oxidized, with as result the existence of an oxidized internal surface (iron oxide grey too) instead nodular graphite.

Compression curves

The four {stress versus deformation} curves are displayed together in the graph presented in Figure 4. One can see that the higher stiffness (slope of the elastic part of the curve, characterized by a Young's modulus) is the one of the pearlitic SG cast iron issued from air-quenching (1). Before reaching about 1GPa (for about 80kN applied) the plastic part of the deformation is still very low.

This is also the case of the martensitic SG cast-iron resulting from water-quenching (2). This one is less stiff than the pearlitic one while post-quenching annealing slightly decreases a again stiffness (3). The least stiff SG iron is the almost ferritic SG cast iron slowly cooled in closed shut-down furnace (4) the plastic deformation before reaching about 80kN is the greatest among the four compressed samples.

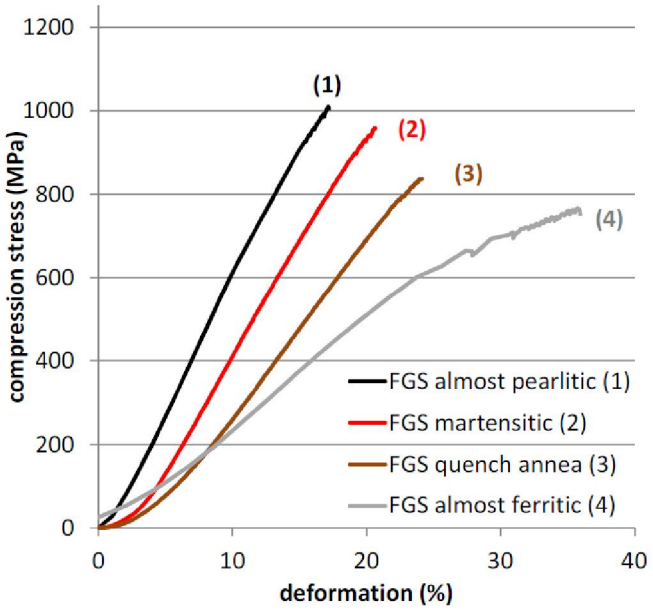

Figure 4 : The four σ =f(ε) compression curves

Plastic deformations achieved

The samples were accurately measured before and after compression. The results are presented in TABLE 1 as well as the resulting relative plastic permanent deformations. One can see that the higher permanent deformation is the one of the almost ferritic sample (-16%)but the almost pearlitic one is also significantly plastically deformed (-13%). The two water-quenched (annealed or not) samples are not plastically deformed (the results, curiously positive, are in the error interval).

Volume masses

The volume masses of the four not compressed samples and of their homologues after compression are graphically presented in Figure 5. One can see first (Figure 5 top) that the volume mass is significantly higher for the ferrite-pearlitic matrixes than for the two martensitic ones which are obviously much less dense (Figure 5, A). Even it is not significant regarding the evolution amplitudes by comparison to the error bars (standard deviation from four values) it seems that a more pearlitic structure may favour a slightly higher density while annealing of martensite also seems inducing a slight increase in density.

Microstructures after compression

The samples were metallographically observed again after compression. The optical micrographs acquired before and after Nital etching, are presented, together with ones taken in the cube centre before compression for comparison, in Figure 6 for the almost ferritic sample, Figure 7 for the almost pearlitic sample, Figure 8 for the martensitic sample and Figure 9 for the annealed martensitic sample.

One can see that, in each case, no microstructure consequence of compression can be detected.

Hardness

Three Vickers indentations under 30kg were

TABLE 1 : Thicknesses of the four samples before and after compression; corresponding relative plastic deformations

Matrix	Ferrite	Pearlite	Martensite	Annealed
Average thickness before compression test (mm)	4.7475	5.115	4.9925	5.3525
Average thickness after compression test (mm)	4.005	4.445	5.075	5.4275
Permanent deformation (%)	-15.6	-13.1	*1.7*	*1.4*

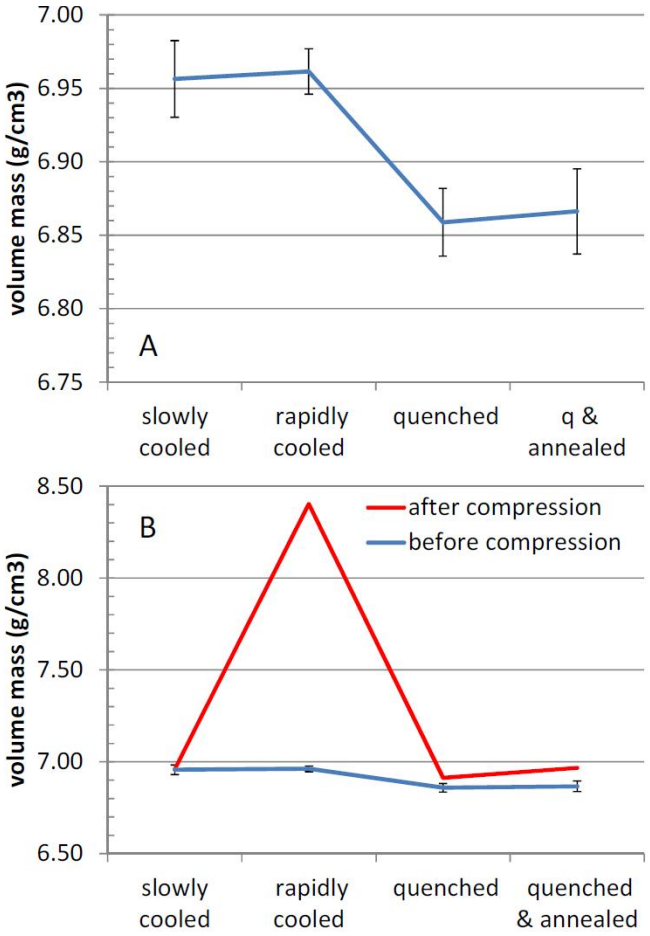

Figure 5 : Volume mass versus matrix's nature (A); influence of the plastic deformation in compression (B)

realized on all samples, with in each case the determination of an average value and a standard deviation one. The obtained results are graphically presented in Figure 10. The hardness logically increases from the almost ferritic sample to the almost pearlitic one, and from the second one to the martensitic sample. Annealing of the later induces a limited but significant softening. The values preliminary obtained on ground and polished surfaces before cutting are globally the lowest ones since because the high temperature oxidation occurred during the austenitization stage which impoverished a little the subsurface of the samples. Concerning the indentation results on the centres of the samples (after cutting), the plastic deformation resulted in a significant hardening only for the almost ferritic sample while not so important effect was observed for the almost pearlitic sample. Curiously the consequences seemed to be inverse for the two martensitic structures.

General commentaries

All these samples issued from the same initial ingot, thus presenting the same chemical composition and the same graphite characteristics, thus constituted of the same spheroidal graphite cast iron,

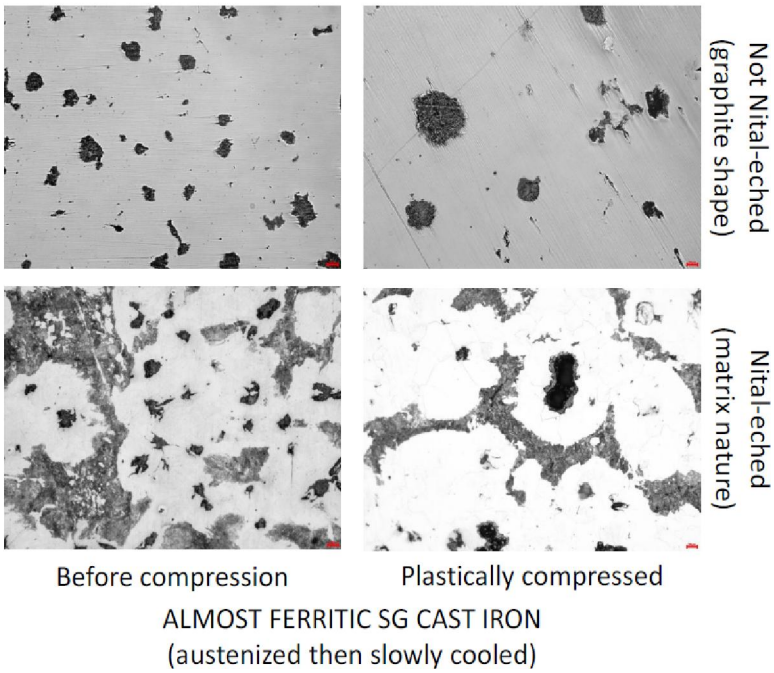

Figure 6 : Graphite structure (without etching, top) and matrix (after Nital etching, bottom) of the sample slowly cooled after austenitization (centre of the cube)

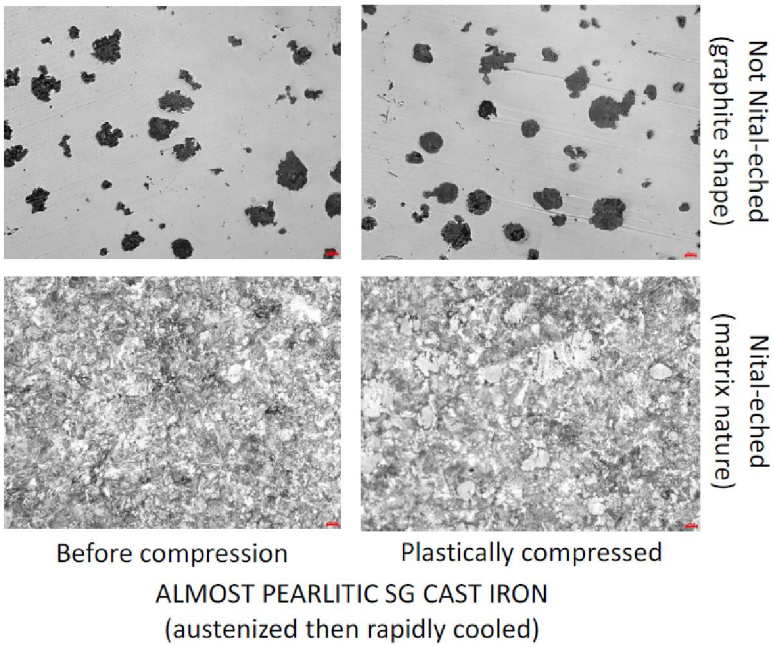

Figure 7 : Graphite structure (without etching, top) and matrix (after Nital etching, bottom) of the sample rapidly cooled after austenitization (centre of the cube)

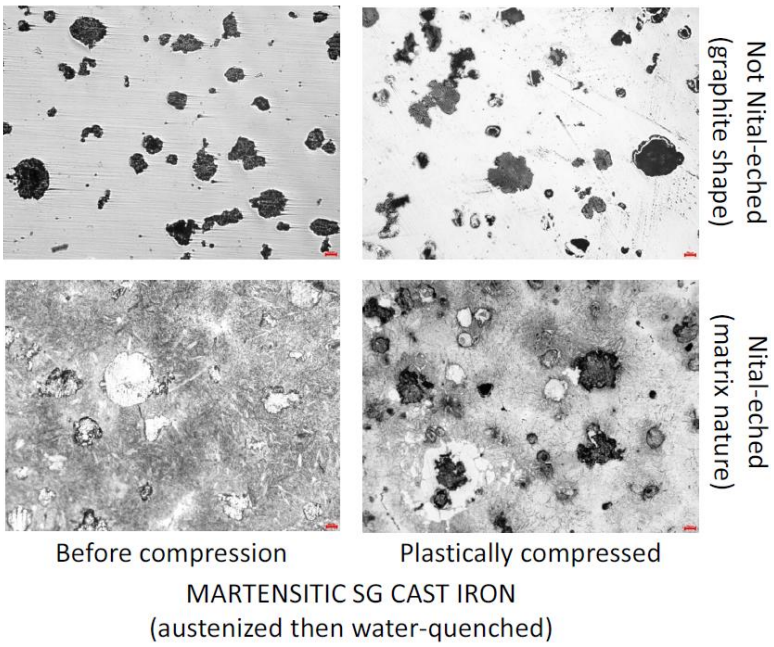

Figure 8 : Graphite structure (without etching, top) and matrix (after Nital etching, bottom) of the sample water-quenched after austenitization (centre of the cube)

were subjected to four different heat treatments to modify their matrix. The initial carbide and pearlite areas disappeared during the high temperature austenitization stage and the cooling conditions led to different matrixes. The major differences obtained concerned logically the hardness (ferritic stucture particularly soft, pearlitic structure significantly harder, martensitic structure much harder than the previous ones, softening effect of the annealing of martensite) but also the densities. The almost pearlitic sample was a little denser than the almost ferritic one while, which can be explained by a greater part of carbon involved in dense cementite carbides inside pearlite and less carbon in not dense graphite. The displacive transformation leading to martensite inversely led to less dense structure, but an-

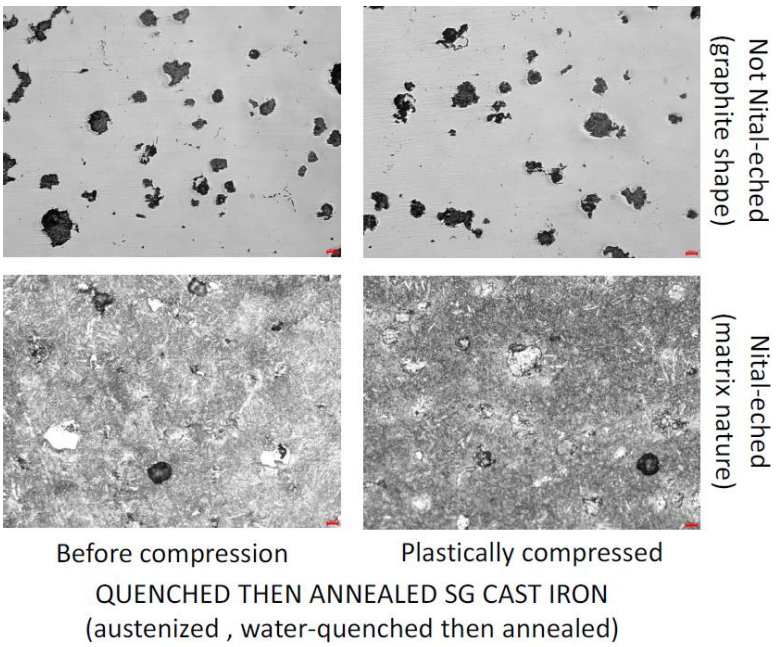

Figure 9 : Graphite structure (without etching, top) and matrix (after Nital etching, bottom) of the sample water-quenched after austenitization and annealed (centre of the cube)

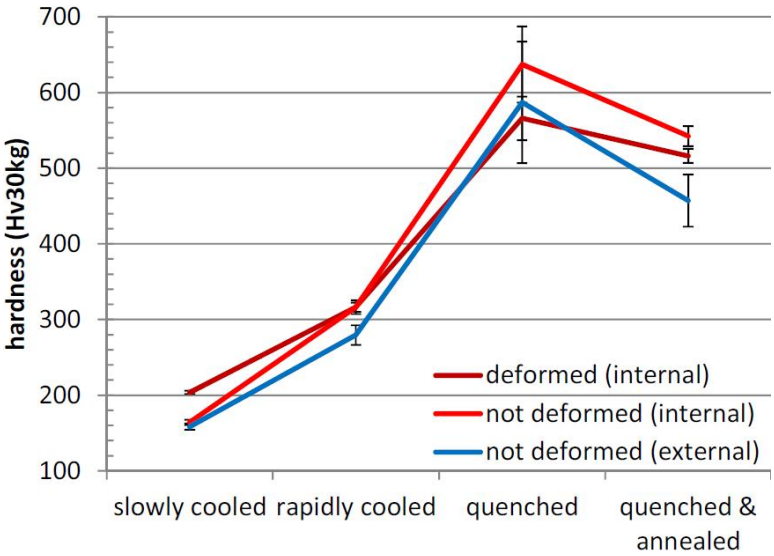

Figure 10 : Hardness in the centres of the samples versus matrix and deformation

nealing, which destabilized a little martensite, induced a limited return to equilibrium structures with as consequence an increase in density. One also saw that stiffness was qualitatively the highest for the carbide-reach pearlitic sample than for the other samples, and even than for the two quenched structures. Annealing induced a slight decrease in stiffness for the water-quenched sample and the ferritic sample was unsurprisingly the less stiff one. These qualitative informations cannot be enriched by quantitative data since no extensometer was available for accurately measure sample contraction.

The deformation during the compression tests were essentially elastic and then no permanent but a significant part of plastic deformation was obtained for the same maximal applied load (about 80kN for all compression tests) for the two ferrite-pearlitic samples only. Except when ferrite was significantly present in the structure these deformation did not really harden the material. Seemingly the microstructures were never changed by these compression runs, even when a significant plastic deformation was

added to the elastic one. Notably the very weak graphite nodules seemed not deteriorated, although that one possibly thought that they were especially deformed during the tests. It is possible that they behave only elastically, with as result an not changed shape when the load was no longer applied.

CONCLUSIONS

Thus, after having generated different microstructures from the same initial material (identical chemical composition and nodule counts) and applied different compression rates for a given maximal load, the classical results were found again, concerning stiffness, hardness or plastic deformation amounts. Consequences were also revealed concerning less classical characteristics such as volume mass. The particular behaviour during compression of the graphite nodules was also observed. This may be of importance for the use of heat-treated SG cast irons. Work extension will now concern impact on the corrosion behaviour for example. This will be matter of future work.

REFERENCES

[1] J.R.Davis; Cast Irons, ASM International, **(1996)**.
[2] G.Lesoult; Traîté des matériaux : Tome 5, Thermodynamique des matériaux : De l'élaboration des matériaux à la genèse des microstructures, Presses Polytechniques et Universitaires Romandes, **(2010)**.
[3] W.F.Gale, T.C.Totemeier; Smithells metals reference book, Elsevier butterworth-heinemann, Burlington, **(2004)**.
[4] J.Szekely; Blast furnace technology, Science and Practice, Dekker, **(1972)**.
[5] J.Szekely, J.W.Evans, H.Y.Sohn; Gas-solid reactions, Academic Press Inc., New York, **(1976)**.
[6] M.Durand-Charre; La microstructure des aciers et des fonts, Genèse et interprétation, SIRPE, Paris, **(2003)**.
[7] M.Durand-Charre; Microstructure of steels and cast irons – engineering materials and processes, Springer-Verlag, Berlin Heidelberg New York, **(2004)**.
[8] G.Béranger; Le livre de l'acier, Lavoisier, Paris Cachan, **(1994)**.
[9] J.R.Davis; Cast irons, ASM International, **(1996)**.
[10] G.Lesoult; Traîté des matériaux : Tome 5, Thermodynamique des matériaux : De l'élaboration des matériaux à la genèse des microstructures, Presses Polytechniques et Universitaires Romandes, **(2010)**.